# Quantitative measurements of Ostwald ripening using time-resolved small-angle neutron scattering

S. Egelhaaf,[1,*] U. Olsson,[2] P. Schurtenberger,[3] J. Morris,[2,†] and H. Wennerström[2]
[1]*ILL, Box 156, F-38042 Grenoble Cedex 9, France*
[2]*Physical Chemistry 1, Center for Chemistry and Chemical Engineering, Lund University, Box 124, S-221 00 Lund, Sweden*
[3]*Institut für Polymere, ETH Zürich, CH-8092 Zürich, Switzerland*
(Received 12 February 1999)

Using a unique method we present accurate quantitative measurements of the Ostwald ripening of an emulsion system. Time-resolved small-angle neutron scattering monitors the time evolution of the average radius and number density of the emulsion drops. The results qualitatively agree with the current theory of Ostwald ripening but there is a quantitative, experimentally significant, discrepancy of a factor of 1.7. We argue that these accurate experiments, performed on a well characterized system, provide a most useful basis for testing further refinements of the theory. [S1063-651X(99)17210-6]

PACS number(s): 82.70.Kj, 61.12.−q, 64.75.+g

Ostwald ripening is a central process in the aging of many two phase systems. In colloidal systems it causes a time dependence of the properties of sols, emulsions, and foams. It is an unwanted process in most applications, but it can also be turned into an advantage to produce nearly monodisperse latex particles [1].

The basic mechanism of Ostwald ripening involves the diffusion of individual molecules from smaller aggregates to larger ones driven by the difference in the relative magnitude of the surface free energy [2]. Lifshitz and Slyozov [3] and independently Wagner [4] developed a theory describing the main features of the process. A central result is that asymptotically the mean particle radius $R$ varies with time, $t$, as

$$R(t)=\left(\frac{8\gamma D c_{\mathrm{eq}} V_M^2}{9kT}\right)^{1/3} t^{1/3}, \tag{1}$$

where $\gamma$ is the surface free energy (surface tension), $c_{\mathrm{eq}}$ the molecular equilibrium concentration of the dispersed phase in the medium, $D$ its diffusion coefficient there, and $V_M$ its volume. Later theoretical efforts [5–7] have confirmed this basic result and extended it to finite volume fractions, $\phi$, of the dispersed phase with an additional correction factor to the proportionality constant in Eq. (1)

$$\alpha=1+0.74\phi^{1/2}. \tag{2}$$

The considerable theoretical effort put into the analysis of the Ostwald ripening process has not been matched by experimental results to quantitatively test the predictions. Experimentally, an Ostwald ripening process can often be identified by studying the rate dependence on the solubility $c_{\mathrm{eq}}$. Using light scattering measurements the $t^{1/3}$ rate law has been confirmed [8–10]. However, it has turned out to be more problematic to obtain a quantitative agreement between the directly measured proportionality constant in Eq. (1) and the value calculated from independent determinations of the molecular parameters.

In this paper we present a time-resolved small-angle neutron scattering (SANS) study of an Ostwald ripening process in a well characterized emulsion system composed of water, decane, and the nonionic surfactant pentaethylene glycol dodecylether ($C_{12}E_5$). At a surfactant-to-oil volume fraction ratio of $\phi_s/\phi_o=0.815$, a water-rich (oil-in-water) microemulsion phase is stable in the temperature range from 25 to 32 °C, while below 25 °C the microemulsion phase separates with a pure oil as the second phase [11]. The temperature dependence of the phase equilibria arises from a strong temperature dependence of the surfactant monolayer spontaneous curvature [12]. At the phase boundary at 25 °C, which is remarkably independent on water concentration, the solution consists of spherical microemulsion oil droplets corresponding to the maximum curvature towards oil given the constraint of the area-to-enclosed volume ratio imposed by the ratio $\phi_s/\phi_o$ [12]. The radius is approximately 75 Å, the polydispersity low, and structural and dynamical properties follow closely those of a hard sphere fluid [13]. When the temperature is decreased below 25 °C the preferred curvature towards oil increases and when equilibrium is reached the microemulsion droplets have decreased in size and an excess oil phase has appeared.

Let us now consider the dynamic process by which oil is removed from the microemulsion phase when a sample originally in the equilibrium state of spherical droplets is rapidly temperature quenched into the two phase area. To reach the new equilibrium state the oil phase has to nucleate. From turbidity experiments we have evidence that this is a homogeneous nucleation process [14,15]. The mechanism involves the growth of some of the droplets allowing the majority of droplets to decrease in size (Fig. 1). The free-energy changes in this process are dominated by the curvature energy of the film. It was established both theoretically and through turbidity experiments that for moderate quenches a barrier for the nucleation exists, while for deeper temperature quenches the system is locally unstable [15].

*Present address: Department of Physics and Astronomy, The University of Edinburgh, Mayfield Road, Edinburgh EH9 3JZ, United Kingdom.
†Present address: Zeneca Agrochemicals, Formulation Group, Jealott's Hill Research Station, Bracknell, Berkshire RG42 6EY, United Kingdom.

 

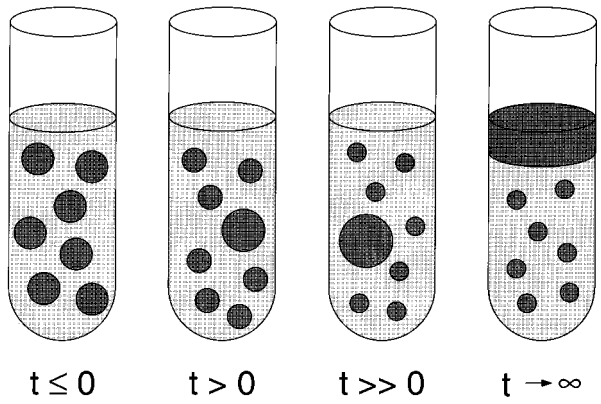


FIG. 1. At $t=0$ an equilibrium system of oligodisperse oil-in-water microemulsion droplets is quenched into a two phase area where, at final equilibrium ($t=\infty$), smaller droplets coexist with an excess oil phase. The oil phase nucleates at a few of the initial droplets which subsequently grow ($t>0$), allowing the majority of droplets to decrease in size.

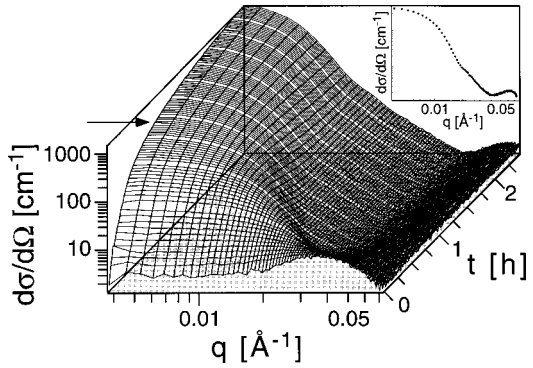


FIG. 2. Sequence of scattering curves from a time-resolved small-angle neutron-scattering experiment recorded during the nucleation and growth of an excess oil phase from oil-in-water microemulsion droplets. For clarity, only every second measurement is shown. As an example the scattering curve obtained at $t=52$ min is added as an inset.

However, while turbidity measurements may report on the onset of nucleation, SANS is much better suited to follow the phase separation process in more detail and to obtain quantitative structural information.

The fraction of the initial droplet population that grows in size is small and in order to experimentally detect this fraction already at early stages we have utilized contrast matching to reduce the forward scattering intensity from the small microemulsion core-shell droplets. Initially they have a radius $R_1=68$ Å, composed of $d_{22}$-decane, covered by a shell of $C_{12}F_5$ having a thickness $\delta=15$ Å. The average scattering length density of these droplets can be matched by dissolving them in an appropriate mixture of $D_2O$ and $H_2O$. Here we used a $H_2O$ volume fraction of 0.355. In this case the scattered intensity from the microemulsion droplets is very small for $q<0.02$ Å$^{-1}$ allowing us to monitor a small fraction of growing drops.

The small-angle neutron-scattering experiments were performed on the instrument D22 at the ILL, Grenoble. This instrument is particularly suited for time-resolved experiments due to the high neutron flux and the large area detector, which in addition can be offset, giving a large scattering vector coverage within a single detector setting [16]. The detector was positioned so that we could follow both the evolution of growing emulsion drops at lower $q$, where the scattering of the small droplets was suppressed, as well as the decrease in size of the smaller droplets indicated by the form factor maximum at $q\approx0.04$ Å$^{-1}$. The sample was temperature quenched into the unstable regime at 13 °C where the equilibrium droplet radius in the microemulsion is 45 Å. Scattering curves were measured for periods of 30 s over an observation period of more than 2 h as shown in Fig. 2.

Dramatic changes in the scattering occur as time progresses particularly at low $q$ values. The growing scattering intensity at low $q$ values is due to the increasing contribution from the few large drops. The large drops retain an oligodisperse ($\sigma_R\approx0.3$) size distribution as can be seen qualitatively from the ''hump'' in the scattering curves, which at later times appears at $q\approx0.02$ Å$^{-1}$ corresponding to the second peak in the form factor of a sphere. This is seen in the inset in Fig. 2 which shows the scattering curve obtained at $t=52$ min. Apart from the first 20 minutes or so, the scattering at low $q$ is completely dominated by the contribution from the large drops. The concentration of the large drops is so low that their relative positions are uncorrelated, and we can also neglect interference effects between large and small droplets due to the size difference. Thus, the scattering in the low $q$ regime can be described as arising from a low concentration of large drops dispersed in an essentially continuous solvent made up of water and the small droplets.

A Guinier analysis [17] yields the time evolution of the radius of gyration $R_{g,\mathrm{big}}$ of the large drops. The $R_{g,\mathrm{big}}$ values were converted to sphere radius, $R_{\mathrm{big}}$, using the known scattering length densities of surfactant ($\rho_s=0.13\times10^{10}$ cm$^{-2}$), oil ($\rho_o=6.54\times10^{10}$ cm$^{-2}$), and water ($\rho_w=4.23\times10^{10}$ cm$^{-2}$), where the latter corresponds to a $H_2O$ volume fraction of 0.355. Neglecting polydispersity we have

$$R_{g,\mathrm{big}}^2=\frac{3}{5}\left(\frac{R_{2,\mathrm{big}}^2-AR_{1,\mathrm{big}}^2}{1-A}\right), \tag{3}$$

where

$$A=\left(1-\frac{\rho_o-\rho_w}{\rho_s-\rho_w}\right)\left(\frac{R_{1,\mathrm{big}}}{R_{2,\mathrm{big}}}\right)^3, \tag{4}$$

and $R_{2,\mathrm{big}}=R_{1,\mathrm{big}}+\delta$. In Fig. 3, $R_{\mathrm{big}}$, defined as $R_{\mathrm{big}}=R_{1,\mathrm{big}}+\delta/2$, is plotted as a function of $t^{1/3}$. This emphasizes the fact that the radius of the big droplets grows as the cubic root of time at long times.

From the Guinier analysis we also obtain the forward ($q=0$) scattering cross section, $d\sigma(0)/d\Omega$. For our core-shell spheres this is given by [17]

$$\frac{d\sigma}{d\Omega}(0)=\frac{N_{\mathrm{big}}}{V}\left(\frac{4\pi}{3}[(\rho_s-\rho_w)R_{2,big}^3+(\rho_o-\rho_s)R_{1,big}^3]\right)^2, \tag{5}$$

where $N_{\mathrm{big}}/V$ is the number density of drops. Thus, by using Eq. (5), we can obtain the time variation of $N_{\mathrm{big}}/V$ from the time variations of $R_{\mathrm{big}}$ and $d\sigma(0)/d\Omega$. In Fig. 4 $N_{\mathrm{big}}/V$ is

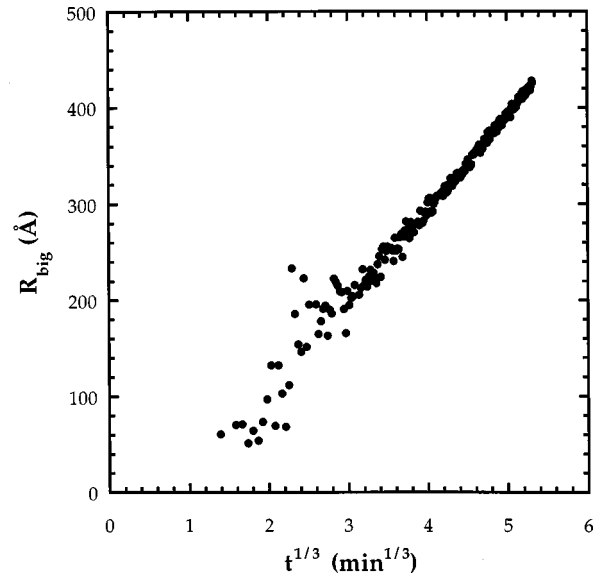


FIG. 3. Time dependence of the big drop radius $R_{big}$ as obtained from a Guinier fit of the data in Fig. 2.

plotted as a function of $1/t$. Apart from the early times where also the statistics were less accurate, the relationship is approximately linear.

Due to the large $q$ range we not only obtain information on the growth of the large drops, but can in addition monitor the decrease in size of the small droplets. The local maximum in the scattering curves of Fig. 2 initially found at $q \approx 0.04\,\text{Å}^{-1}$ reflects the size of the small droplets. As time progresses, it moves to higher $q$ values as the microemulsion droplets decrease in size. However, after about 45 min the maximum has reached a stable position at $q \approx 0.065\,\text{Å}^{-1}$ corresponding to the equilibrium radius $R_{small} \approx 45$ Å at 13 °C.

The shrinkage of the small droplets from 75 to 45 Å implies that totally 40% of the oil, initially present in the microemulsion, is removed at equilibrium. At $t = 45$ min the radii of the big drops have reached 250 Å. The initial oil volume fraction was 0.055 and when the small droplets have equilibrated the volume fraction of big droplets is approximately 0.025. For $R_{big} = 250$ Å, this corresponds to a number density of $4 \times 10^{14}\,\text{cm}^{-3}$, which is in good agreement with the measured value of $N_{big}/V$, providing a consistency test of the analysis and interpretation of the scattering data. Thus, there is an initial phase ending at $t \approx 45$ min where the big drops form and grow at the cost of the small droplets. At this time all the oil of the emerging bulk phase is present in the larger drops, and they form an emulsion system which is aging by Ostwald ripening.

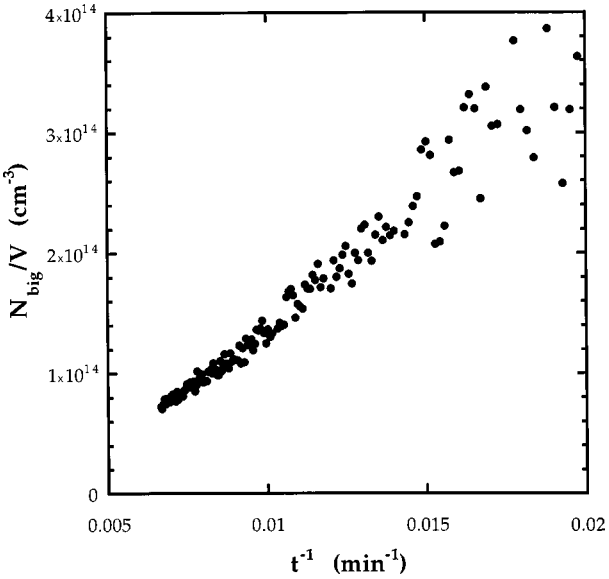


FIG. 4. Time dependence of the number density of large drops as determined from the extrapolated scattering intensity at $q = 0$ and the average radius obtained from the Guinier fit.

In Eqs. (1) and (2) we have a prediction for the absolute rate of the ripening process in terms of independently measurable parameters. For the surface tension $\gamma$ the dominant contribution comes from the curvature free energy, $G_C$ of the surfactant film which varies with drop radius as

$$G_c = 8\pi\kappa'(1 - Rc_0)^2, \tag{6}$$

where $\kappa' = \kappa + \bar{\kappa}/2$ is a combination of the bending $\kappa$ and saddle splay $\bar{\kappa}$ modulii and $c_0$ is the preferred curvature [15]. Equation (6) represents a size dependent surface free energy and for large radii, $Rc_0 \gg 1$, we find

$$\gamma = 2\kappa' c_0^2. \tag{7}$$

In independent measurements on the equilibrium system [18] we have determined that $\kappa' = 6 \times 10^{-21}$ J and with $c_0 = 1/45\,\text{Å}^{-1}$ at $T = 13\,°\text{C}$ this yields $\gamma = 0.6\,\text{mJ/m}^2$. The other two system specific parameters entering Eq. (1), the decane diffusion coefficient and solubility $c_{eq}$ in water, are difficult to measure directly due to the low solubility, but they can be estimated with a reasonable accuracy by extrapolating from values for shorter hydrocarbons. In this way we arrive at $D \approx 7 \times 10^{-10}\,\text{m}^2\,\text{s}^{-1}$ [19] and $c_{eq} \approx 2 \times 10^{20}\,\text{m}^{-3}$ [20]. Combining these values and using Eq. (2), ($\alpha = 1.12$) to correct for the finite concentration of drops we arrive at the theoretical estimate of $1.5 \times 10^{-9}\,\text{m}\,\text{s}^{-1/3}$ for the slope of the line in Fig. 3, while the experimental value is $2.5 \times 10^{-9}\,\text{m}\,\text{s}^{-1/3}$.

The time-resolved SANS experiments provide accurate data on the initial formation and subsequent growth of oil drops nucleated after a temperature quench of an oil-in-water microemulsion into a two phase region. For the first time we have access to the simultaneous temporal evolution of the size distribution of oil drops and small microemulsion spheres, which allows for a detailed, quantitative description of the processes. Right after the temperature quench there is a fast nucleation process followed by a phase where these nuclei grow by diffusion of oil from the small droplets. After approximately 45 min the small droplets have reached their (near) equilibrium size and the large drops continue to evolve through Ostwald ripening at constant oil volume. From the measured intensity at $q = 0$ we not only verify that the number of drops decrease with time as $t^{-1}$ but we also obtain a quantitative measure of the drop concentration. Independently the Guinier analysis provides the temporal evolution of the mean drop radius which displays a $t^{1/3}$ growth law at longer times consistent with the $N_{big}/V$ data. Moreover, the system is sufficiently well characterized that we can make a theoretical estimate of the slopes of Figs. 3 and 4. In

view of the fact that we perform an *a priori* analysis of a dynamic process in a complex liquid, the discrepancy of a factor of 1.7 between the measured and predicted slope of Fig. 3 appears to be quite reasonable. A similar discrepancy between theory and experiment has been observed previously based on light scattering studies of the Ostwald ripening (see, e.g., Ref. [8]). However, the time-resolved SANS experiments on a very well characterized model system have provided us with a unique set of data, and the prediction is clearly outside the margin of random errors. Currently the theoretical description of Ostwald ripening does not account for the Brownian motion of the drops themselves, for the size dependence of the surface tension, which is described by Eq. (7), and, particular to emulsion systems, the contribution to molecular transport from the small droplets (micelles) [21]. The present system is sufficiently well characterized that all these features can be described accurately by themselves. We thus believe that we now have a sound basis for further refinements of the theory and are in a position to aim for a unified description of the Ostwald ripening that takes all these additional features into account.

We acknowledge the Institut Laue-Langevin, Grenoble, France, for providing the neutron scattering facilities. This work was supported by the Swedish Natural Science Research Council (NFR) and the Göran Gustafsson Foundation.

[1] J. Ugelstad, P. C. Mørk, K. H. Kaggerud, T. Ellingsen, and A. Berge, Adv. Colloid Interface Sci. **13**, 101 (1980).
[2] W. Ostwald, Z. Phys. Chem., Stoechiom. Verwandtschaftsl. **34**, 295 (1900).
[3] I. M. Lifshitz and V. V. Slyozov, Zh. Eksp. Teor. Fiz. **35**, 479 (1958) [Sov. Phys. JETP **35**, 331 (1959)].
[4] C. Wagner, Z. Elektrochem. **65**, 581 (1961).
[5] P. W. Voorhees, J. Stat. Phys. **38**, 231 (1985).
[6] A. D. Brailsford and P. Wynblatt, Acta Met. **27**, 489 (1979).
[7] J. A. Marquisee and J. Ross, J. Chem. Phys. **79**, 373 (1983).
[8] A. S. Kabalnov, K. N. Makarov, A. V. Pertsov, and E. D. Shchukin, J. Colloid Interface Sci. **138**, 98 (1990).
[9] P. Taylor and R. H. Ottewill, Colloids Surf., A **88**, 303 (1994).
[10] J. G. Weers and R. A. Arlauskas, Langmuir **11**, 474 (1995).
[11] M. L. Leaver *et al.*, J. Chem. Soc., Faraday Trans. **91**, 4269 (1995).
[12] U. Olsson and H. Wennerström, Adv. Colloid Interface Sci. **49**, 113 (1993).
[13] U. Olsson and P. Schurtenberger, Prog. Colloid Polym. Sci. **104**, 157 (1997).
[14] J. Morris, U. Olsson, and H. Wennerström, Langmuir **13**, 606 (1997).
[15] H. Wennerström, J. Morris, and U. Olsson, Langmuir **13**, 6972 (1997).
[16] S. U. Egelhaaf and P. Schurtenberger, Physica B **234-236**, 276 (1997).
[17] J. S. Pedersen, Adv. Colloid Interface Sci. **70**, 171 (1997).
[18] T. D. Le, U. Olsson, H. Wennerström, and P. Schurtenberger, Phys. Rev. E (to be published).
[19] W. Hayduk and H. Laudie, AIChE. J. **20**, 611 (1974).
[20] C. McAuliffe, J. Phys. Chem. **70**, 1267 (1966).
[21] A. S. Kabalnov, Langmuir **10**, 680 (1994).